Impact of aerosols and atmospheric thermodynamics on cloud properties within the climate system

Toshihisa Matsui, Hirohiko Masunaga, and Roger A. Pielke Sr.
Department of Atmospheric Science, Colorado State University, Ft. Collins, Colorado, USA

Wei-Kuo Tao
Laboratory for Atmospheres, NASA Goddard Space Flight Center, Greenbelt, Maryland, USA

Received 15 December 2003; revised 27 January 2004; accepted 19 February 2004; published 18 March 2004.

[1] A combination of cloud-top and columnar droplet sizes derived from the multi Tropical Rainfall Measurement Mission (TRMM) sensors reveals the sensitivity of the aerosols effect on cloud-precipitation processes due to environmental vertical thermodynamic structure. First, the magnitude of aerosol indirect effect could be larger with the analysis of columnar droplet sizes than that derived from the cloud-top droplet sizes since column-droplet size can account for the broader droplet spectra in the cloud layers. Second, a combination of cloud-top and columnar droplet sizes reveals that the warm rain process is prevented regardless of the aerosols concentration under high static stability such as when a strong temperature inversion exists, while a high aerosol concentration suppresses the warm rain formulation under low static stability. *INDEX TERMS:* 0305 Atmospheric Composition and Structure: Aerosols and particles (0345, 4801); 0320 Atmospheric Composition and Structure: Cloud physics and chemistry; 1610 Global Change: Atmosphere (0315, 0325); 1640 Global Change: Remote sensing.
Citation: Matsui, T., H. Masunaga, R. A. Pielke Sr., and W.-K. Tao (2004), Impact of aerosols and atmospheric thermodynamics on cloud properties within the climate system, *Geophys. Res. Lett.*, *31*, L06109, doi:10.1029/2003GL019287.

1. Introduction

[2] Maritime low clouds, denoted hereafter as stratus, reduce the Earth's energy budget by approximately 15 (W/m^2) in an annual average through an imbalance between the longwave emission and the reflection of solar radiation [*Hartmann et al.*, 1992]. This large impact of stratus to the Earth's radiation budget has motivated studies to examine the factors governing the microphysical properties of stratus.

[3] Stratus amount is, in particular, positively correlated with *lower-tropospheric static stability* (LTSS), defined as the potential temperature difference between the surface and the 700 (mb) pressure level [*Klein and Hartmann*, 1993]. *Klein and Hartmann* [1993] demonstrate that high LTSS represents a strong temperature inversion at the top of the atmospheric boundary layer, and the regional observations show that the stratus cloud is confined to the boundary layer in high LTSS, while extending their horizontal areal coverage.

[4] *Aerosols* also control stratus properties by acting as cloud condensation nuclei (CCN) to form cloud droplets. A high concentration of the aerosols overseed cloud droplets to generate highly concentrated, narrowly distributed cloud droplet spectra, which increase the cloud albedo up to 30% [*Twomey et al.*, 1984]. Narrowly distributed cloud droplet spectra prevent the formulation of precipitation and could increase the cloud lifetime that further cools the Earth's surface [*Albrecht*, 1989]. This climatic impact of aerosols on cloud properties is called the aerosol indirect effect, which is one of the largest uncertainties in accurately describing the sensitivity of climate to changes in aerosol concentrations in the future.

[5] Figure 1 exhibits a global distribution of seasonally-averaged LTSS (color contours) derived from the NCEP/NCAR Reanalysis [*Kalnay et al.*, 1996] and seasonally-averaged aerosol index derived from the MODerate resolution Imaging Spectroradiometer (MODIS) (dark shaded) [*Tanré et al.*, 1997]. The aerosol index is better correlated than aerosol optical depths with the column aerosol concentrations under some assumptions [*Nakajima et al.*, 2001], and was derived from the aerosol optical thickness at 0.55 (μm) and Ångstrom exponent computed from 0.55 and 0.865 (μm). Different contributions from these two factors across the globe possibly influence the cloud microstructure. This paper examines the sensitivity of the aerosol effect to the cloud properties on a global scale due to the background atmospheric thermodynamic structure.

2. TRMM-Derived Cloud Properties

[6] A new algorithm using the Tropical Rainfall Measurement Mission (TRMM) Microwave Imager (TMI) and Visible/Infrared Radiance Imager (VIRS) provides the vertical structure of warm cloud (cloud top temperature >273 K) microstructure by investigating two types of droplet effective radius (Re): shortwave-derived droplet size (Re (top)) and microwave-derived droplet size (Re (column)). This is because a VIRS-derived Re tends to be biased toward a cloud-top value due to strong absorption of the near-infrared band, whereas a TMI-derived Re is expected to be close to the value averaged over the cloud layer since microwave can detect cloud droplets and rain drops without suffering from saturation within low maritime clouds. Partial cloudiness in a large TMI footprint is corrected by VIRS-derived cloud fraction [*Masunaga et al.*, 2002a].

[7] Figure 2 shows the relationship between seasonally averaged (March–May) Re (top) and Re (column) at each grid between 37°N and 37°S. Re (top) generally ranges from 10 to 21 (μm), whereas Re (column) broadly ranges up

0094-8276/04/2003GL019287

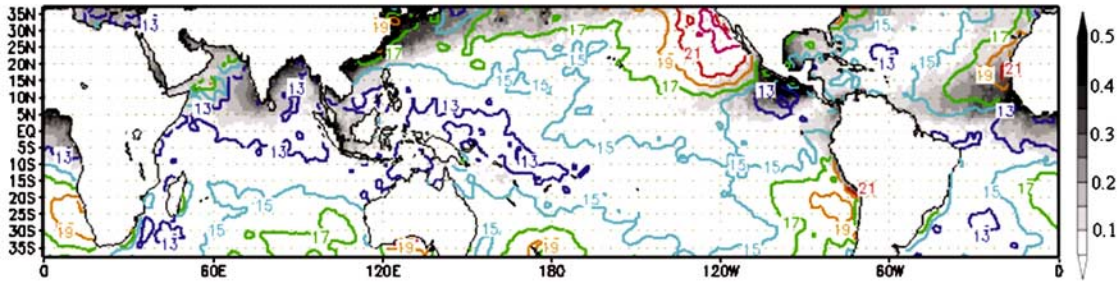

Figure 1. Global distribution of aerosol index (dark shaded) from the MODIS measurements and lower-tropospheric static stability (LTSS) (K) (colored contour) derived from the NCEP/NCAR Reanalysis averaged through March–May 2000.

to 40 (μm). Re (top) is generally larger than that derived from the *Bréon et al.* [2002], since optically thin, broken clouds (less than 30% of TMI footprint) were omitted from our analysis in order to reduce the error associated with the surface emissivity in microwave analysis. Figure 2 can be used to judge different cloud modes due to the fact that clouds are likely to exhibit significant droplet growth when Re exceeds 15 (μm) [see *Masunaga et al.*, 2002b, and references therein]. A cloud with both Re (top) and Re (column) < 15 (μm) in the zone-I is assigned as *non-precipitating*, since the cloud is not drizzling with Re (column) < Re (top); i.e., cloud droplet sizes increase toward the cloud top. Clouds with Re (top) > 15 (μm) and Re (column) < 15 (μm) in the zone-II are assigned as *transitional*, since the droplets increase in size toward the cloud top where drizzle drops have begun to form. Clouds with Re (top) > 15 (μm) and Re (column) > 15 (μm) in the zone-III are assigned as *precipitating*, since the cloud is drizzling with Re (column) > Re (top); i.e., droplet sizes increase toward the cloud base, indicating the presence of larger precipitation-size droplets in that area. In a small number of clouds, Re (column) is greater than the Re (top), although Re (top) does not exceed the drizzle threshold. Clouds in zone-IV are assigned as *uncertain*.

[8] Figure 3a shows a global map of four cloud modes by overlaying the global distribution of Re (column) and Re (top) with a color coordination to represent the degree of the cloud mode (Figure 3b). Non-precipitating stratus (red) exists downwind of continents. Those regions are generally characterized with polluted (a high aerosol index) and/or stable atmosphere (high LTSS) (Figure 1). The stratus in the rest of the subtropical regions characterized with relatively polluted and moderately stable atmosphere is in the transitional mode (green). Transitional stratus is also found in the Inter Tropical Convergence Zone and the Pacific Warm Pool where deep cumulus convection (cold-rain process) promotes a subsidence in the surrounding warm clouds.

[9] Precipitating stratus (blue) is found in the outer fringes of the tropical rain area. These regions, compared to the regions with non-precipitating stratus, are generally characterized with pristine and/or less stable atmosphere (Figure 1). The areas with precipitating clouds correspond to the warm rain regions observed by the TRMM Precipitation Radar [*Schumacher and Houze*, 2003]. Uncertain stratus (black) is present in a small portion of the north Indian Ocean and Caribbean Sea.

3. Sensitivity of the Aerosol Indirect Effect

3.1. Method

[10] Since it is difficult to quantify the relationship from the seasonal mean values, we performed a statistical analysis for the individual estimates of stratus, aerosol index, and LTSS. The three individual datasets are not precisely concurrent in time and space. We directly relate the daily 1-degree MODIS aerosol index, 0.25-degree TRMM cloud properties, and 2.5-degree LTSS from the NCEP/NCAR reanalysis without spatial interpolation. The maximum difference in overpass timing between the TRMM and the MODIS is set to be 3 hours, minimizing the error associated with the different satellite overpasses. The LTSS from the NCEP/NCAR Reanalysis is linearly interpolated for the TRMM overpass timing. The total sampling number of the quasi-coincident observations was 462,289; 287,007 of the total were observed in the subtropical region (25°–37°N and 25°–37°S), while 170,304 of the total were observed in the tropical region (25°S–25°N).

3.2. Results

[11] The means of Re (top) and Re (column) were derived with a given aerosol index (bins of 0.02) and LTSS (bins of 0.4 K) (Figure 4). The three-dimensional slope shows that high aerosol index and/or high LTSS leads to the smaller droplet size in both Re (column) and Re (top); i.e., a larger temperature inversion and higher concentrations of aerosols inhibit cloud droplet growth. On the other hand, cloud

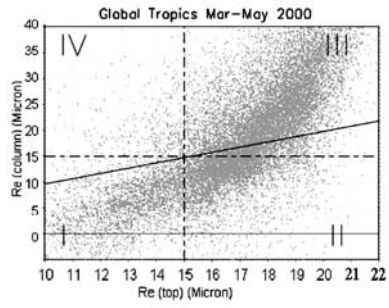

Figure 2. Seasonally averaged Re (top) and Re (column) at each grid box are compared. Dash lines represent 15-micron drizzle threshold. Solid line shows the 1:1 ratio between Re (top) and Re (Column). Re (column) is greater than the Re (top) when clouds are located above the solid line.

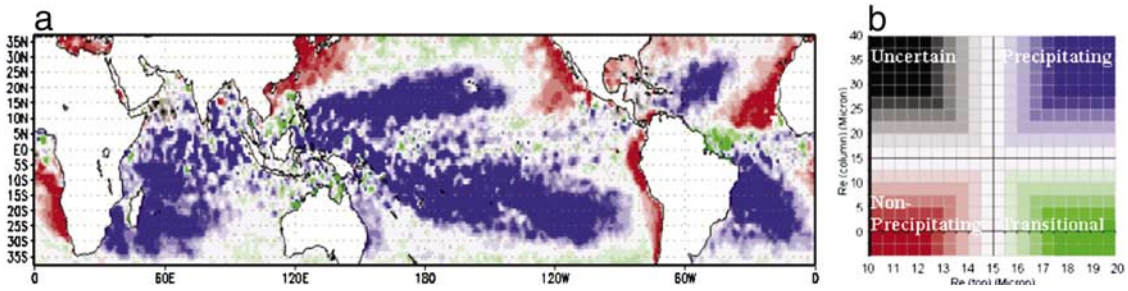

Figure 3. a) Global distribution of non-precipitating (red), transitional (green) and precipitating (blue) modes of warm cloud averaged through March–May 2000. b) Color coordination based on the warm cloud modes.

droplet sizes are maximized in the pristine and less stable atmosphere.

[12] For a fixed liquid water path, the relationship between *Re* and aerosol index is expressed as [e.g., *Bréon et al.*, 2002]

$$\frac{d\ \log(\mathrm{Re})}{d\ \log(AI)} = \frac{\alpha}{3}, \tag{1}$$

where AI is aerosol index, and α approximately relates the aerosol index to the number of cloud droplets (N_c) via $N_c \approx (AI)^{\alpha}$. The slope ($\alpha/3$) is a parameter that simply quantifies the magnitude of the aerosol indirect effect. Since the standard errors ($\sigma/\sqrt{n-2}$, where n and σ are the number of quasi-coincident measurements for each bin and is standard deviation, respectively) are generally larger for the bins of higher aerosol index due to the lack of the sample number, we derived the slope for an aerosol index >0.25. Although our sampling and statistical processes are different from the previous studies in a strict manner, the slope of Re (top) averaged over a full range of LTSS (0.069) is close to that derived from *Bréon et al.* [2002] (0.085) and less than 50% of that derived from *Nakajima et al.* [2001] (0.16). The slope of Re (column) is 0.222, which is three times larger than that of Re (top), and is close to that using a characteristic value, $\alpha = 0.7$ [*Charlson et al.*, 1992]. Since the Re (column) is directly related to the cloud optical depth [*Masunaga et al.*, 2002a], the aerosol indirect effect and associated Earth's cooling effect could be greater than the estimation using cloud-top Re (-0.7–0.2 W/m^2) [*Nakajima et al.*, 2001].

[13] The slopes of Re (column) averaged over the five bins of LTSS range from 0.12 to 0.32 (Table 1). In the same LTSS intervals, the slope of Re (top) range from 0.022 to 0.071. Those contain values derived over land and ocean [*Bréon et al.*, 2002], suggesting that the difference in the slope between land and ocean could be explained by their background thermodynamic structure, in addition to the observational tendency of the specific sensor [*Rosenfeld and Feingold*, 2003]. Except for the lowest LTSS intervals (12.2–13.8), the slope of Re (column) and Re (top) generally decreases toward the higher LTSS (Table 1); i.e., a greater fraction of aerosols are converted into cloud droplets in the lower LTSS. This result is also physically reasonable, since a lower static stability permits a deeper atmospheric boundary layer and stronger updrafts to yield a higher supersaturation, which activate more CCNs thereby decreasing the droplet size [*Feingold et al.*, 2003]. However, the aerosol effect on the cloud albedo and associated Earth's radiation budget is not necessarily stronger in the convectively unstable atmosphere, since cloud areal coverage becomes very small in such regions [*Klein and Hartmann*, 1993]. The different slopes due to the LTSS also explain why the mean slope of Re (top) is smaller than *Nakajima et al.* [2001]; our sampling number is biased

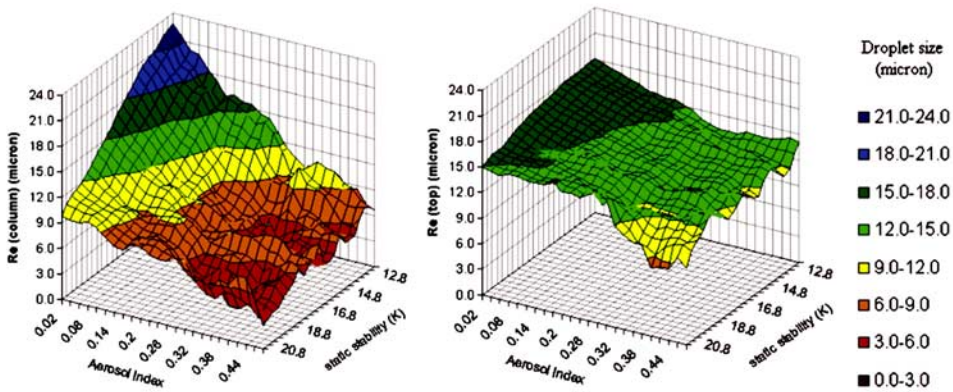

Figure 4. The mean of Re (top) and Re (column) were derived for sets with a given aerosol index (bins of 0.01) and low-atmosphere static stability (bins of 0.4 K) from May to March.

Table 1. The Slope ($\alpha/3$) Averaged Over the Five Bins of the LTSS

Ranges of LTSS (K)	12.2–13.8	14.2–15.8	16.2–17.8	18.2–19.8	20.2–21.8
($\alpha/3$) Re (top)	0.071	0.085	0.084	0.051	0.022
($\alpha/3$) Re (column)	0.19	0.32	0.27	0.20	0.12

toward the subtropical regions, where the LTSS is generally higher than the tropical region.

[14] Finally, Figure 5 provides the distribution of the cloud modes as functions of the aerosol index and the LTSS with the color coordination in Figure 3b. Precipitating stratus (blue) exists when the aerosol index and LTSS are less than approximately 0.08 and 16.8, respectively. Note that the absence of dark blue, which dominates the tropical region in Figure 3, is due to the sampling biases mentioned above. Therefore, Figure 5 should be considered to mainly represent cloud-aerosol interaction in the subtropical region. Non-precipitating stratus (red) exists with a high aerosol index ($\sim$0.24). Transitional stratus (green) lies between the non-precipitating and precipitating stratus. The boundaries of three cloud modes are tilted toward the higher LTSS. Figure 5 clearly shows that a high aerosol concentration suppresses the cloud droplet growth and warm rain process under low static stability; nevertheless, the warm rain process is prevented regardless of aerosol concentration under a high static stability where a strong temperature inversion exists.

4. Summary and Perspectives

[15] Our study demonstrates an important sensitivity of the aerosol effect on the cloud-precipitation process to the different static stability regimes through a simultaneous examination of the cloud-top and columnar droplet effective radius. While the magnitude of its effect of cloud-top values reproduces the value reported in the previous studies, those of columnar values are greater than the previous studies, suggesting a possible underestimation of the aerosol indirect effect with using cloud-top droplet size. The cloud-aerosol interaction is clearly identified except where LTSS is so high that the cloud droplet growth is dynamically suppressed. A further analysis is required for a more quantitative assessment. This study does not account for the vertical distribution of the aerosol concentration. A possible solution is to combine the aerosol dataset from MODIS and a global chemical transport model to distinguish the aerosols above the warm cloud, such as the dust aerosols from the Gobi and Sahara desert [*Ginoux et al.*, 2001]. Indeed, multi-seasonal and multi-year datasets will provide a sufficient sampling number to derive a statistically significant relationship in the specific regions where the chemical compositions of aerosols strongly differ.

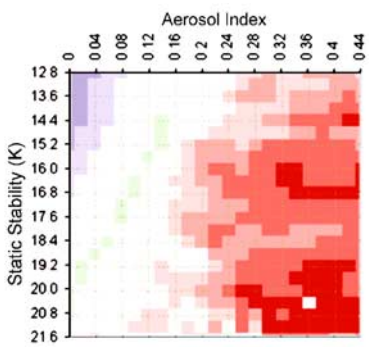

Figure 5. Re (column) and Re (top) are overlaid and colored based on the Figure 3b.

[16] **Acknowledgments.** This work is funded by NASA CEAS fellowship No. NAG5-12105, and NASA Grant No. NNG04GB87G. Wei-Kuo Tao is supported by the NASA Headquarters Atmospheric Dynamics and Thermodynamics Program and the NASA Tropical Rainfall Measuring Mission (TRMM). VIRS (1B01) and TMI (1B11) data were provided by NASA GSFC DAAC. NCEP/NCAR Reanalysis were provided by the NOAA CDC. The authors would like to thank Allen Chu at NASA/GSFC for providing the MODIS aerosol data and T. Y. Nakajima at NASDA/EORC for providing the GTR 4.1 packages. We also thank Dallas Staley for her professional editing.

References

Albrecht, B. A. (1989), Aerosols, cloud microphysics, and fractional cloudiness, *Science*, *245*, 1227–1230.

Bréon, F.-M., D. Tanré, and S. Generoso (2002), Aerosol effect on cloud droplet size monitored from satellite, *Science*, *295*, 834–838.

Charlson, R. J., S. E. Schwartz, J. M. Hales, R. D. Cess, J. A. Coakley Jr., J. E. Hansen, and D. J. Hofmann (1992), Climate forcing by anthropogenic aerosols, *Science*, *255*, 423–430.

Feingold, G., W. L. Eberhard, D. E. Veron, and M. Previdi (2003), First measurements of the Twomey indirect effect using ground-based remote sensors, *Geophys. Res. Lett.*, *30*(6), 1287, doi:10.1029/2002GL016633.

Ginoux, P., M. Chin, I. Tegen, J. Prospero, B. Holben, O. Dubovik, and S.-J. Lin (2001), Sources and global distributions of dust aerosols simulated with the GOCART model, *J. Geophys. Res.*, *106*, 20,255–20,273.

Hartmann, D. L., M. E. Ockert-Bell, and M. L. Michelsen (1992), The effect of cloud type on Earth's energy balance: Global analysis, *J. Clim.*, *5, 1281–1304.*

Kalnay, E., et al. (1996), The NCEP/NCAR 40-year reanalysis project, *Bull. Am. Meteorol. Soc.*, *77*, 437–471.

Klein, S. A., and D. L. Hartmann (1993), The seasonal cycle of low stratiform clouds, *J. Clim.*, *6*, 1587–1606.

Masunaga, H., T. Y. Nakajima, T. Nakajima, M. Kachi, R. Oki, and S. Kuroda (2002a), Physical properties of maritime low clouds as retrieved by combined use of Tropical Rainfall Measurement Mission Microwave Imager and Visible/Infrared Scanner: Algorithm, *J. Geophys. Res.*, *107*(D10), 4083, doi:10.1029/2001JD000743.

Masunaga, H., T. Y. Nakajima, T. Nakajima, M. Kachi, and K. Suzuki (2002b), Physical properties of maritime low clouds as retrieved by combined use of Tropical Rainfall Measurement Mission (TRMM) Microwave Imager and Visible/Infrared Scanner: 2. Climatology of warm clouds and rain, *J. Geophys. Res.*, *107*(D19), 4367, doi:10.1029/2001JD001269.

Nakajima, T., A. Higurashi, K. Kawamoto, and J. E. Penner (2001), A possible correlation between satellite-derived cloud and aerosol microphysical parameters, *Geophys. Res. Lett.*, *28*, 1171–1174.

Rosenfeld, D., and G. Feingold (2003), Explanation of discrepancies among satellite observations of the aerosol indirect effect, *Geophys. Res. Lett.*, *30*(14), 1776, doi:10.1029/2003GL017684.

Schumacher, C., and R. A. Houze Jr. (2003), The TRMM precipitation radar's view of shallow, isolated rain, *J. Appl. Meteorol.*, *42*, 1519–1524.

Tanré, D., Y. J. Kaufman, M. Herman, and S. Mattoo (1997), Remote sensing of aerosol properties over oceans using the MODIS/EOS spectral radiance, *J. Geophys. Res.*, *102*, 16,971–16,988.

Twomey, S. A., M. Piepgrass, and T. L. Wolfe (1984), An assessment of the impact of pollution on global cloud albedo, *Tellus, Ser. B*, *36*, 356–366.

T. Matsui, H. Masunaga, and R. A. Pielke Sr., Department of Atmospheric Science, Colorado State University, Ft. Collins, CO 80523-1371, USA. (matsuit@atmos.colostate.edu)

W.-K. Tao, Laboratory for Atmospheres, NASA Goddard Space Flight Center, Greenbelt, MD 20771, USA.